Journal of Molecular Modeling (2018) 24: 44
https://doi.org/10.1007/s00894-018-3580-4

ORIGINAL PAPER

Theoretical insight into reaction mechanisms of 2,4-dinitroanisole with hydroxyl radicals for advanced oxidation processes

Yang Zhou[1,2] · Xiaoqiang Liu[1] · Weidong Jiang[1] · Yuanjie Shu[1]

Received: 27 October 2017 / Accepted: 5 January 2018 / Published online: 24 January 2018

Abstract

The detailed degradation mechanism of an insensitive explosive, 2,4-dinitroanisole (DNAN), in advanced oxidation processes (AOPs) was investigated computationally at the M06-2X/6–311 + G(d,p)/SMD level of theory. Results obtained show that the addition-elimination reaction is the dominant mechanism. The phenol products formed can continue to be oxidized to benzoquinone radicals that are often detected by experiments and may be the initial reactants of ring-opening reactions. The H-abstraction reaction is an unavoidable competing mechanism; the intermediate generated can also undergo the process of addition-elimination reaction. The nitro departure reaction involves not only hydroxyl radical (•OH), but also other active substances (such as •H). More importantly, we found that AOP technology can easily degrade DNAN, similar to TNT and DNT. Thus, this method is worth trying in experiments. The conclusions of this work provide theoretical support for such experimental research.

Keywords DNAN · Advanced oxidation process · Reaction mechanism · DFT

Introduction

The ecological problems of explosives are attracting more and more attention in many countries [1]. On the other hand, the search for, and use of, new explosives never ceases. For example, to increase the safety of weapons, the development of insensitive munitions (IM) has become a main driving force of modern explosives research. One of the first IM ingredients to be used on a large scale is 2,4-dinitroanisole (DNAN), which offers promise as a replacement for 2,4,6-trinitrotoluene (TNT) in melt-cast explosive formulations [2]. Unfortunately, the toxicity of DNAN almost matches that of TNT [3, 4]. Therefore, the release of DNAN and its production wastewater poses a threat to the ecological environment and public health. Thus, effective methods to remove this pollutant from the environment must be sought, especially considering that early techniques such as incineration, detonation and ocean dumping have been declared dangerous and illegal.

In recent years, advanced oxidative processes (AOPs) have become one of the most promising methods for removing explosives from contaminated soils, sediments and water [5–9]. However, studies on removing DNAN by AOPs are rare, although this method has been shown to be effective for TNT, 2,4-dinitrotoluene (DNT), and so on. Several biodegradation works have evaluated DNAN biotransformation under anaerobic, microaerophilic and aerobic conditions, and some metabolites had also been elucidated [10–13]. Additionally, the alkaline hydrolysis of DNAN has also been investigated by a combination of experimental and theoretical technologies [14–16]. Obviously, as another significant alternative method, the potential of AOPs should not be ignored, especially as they have shown good performance with other explosives [5–9]. Understanding the detailed degradation mechanism of DNAN by AOPs is a crucial precondition to promoting the use of AOP technology for the effective removal of DNAN.

Here, we first explored the reaction mechanism of DNAN with the hydroxyl radical (•OH) in AOPs. Considering the

Yang Zhou and Xiaoqiang Liu contributed equally to this work.

✉ Yang Zhou
zhouy@caep.cn

✉ Yuanjie Shu
1204172675@qq.com

[1] College of Chemistry and Environmental Engineering, Sichuan University of Science and Engineering, Zigong 643000, China

[2] Institute of Chemical Materials, China Academy of Engineering and Physics, Mianyang 621900, China

challenge of capturing lively radicals and short-lived intermediates, we chose density functional theory (DFT) methods for this study. Indeed, the lack of experimental data unavoidably increases the difficulty of this work because of the existence of numerous reaction channels. Fortunately, two previous studies on AOP degradation of TNT and DNT [17, 18] and alkaline hydrolysis of DNAN [14–16] were able to provide valuable reference information. The latter mainly included three pathways for the initial steps: hydrogen abstraction, the formation of Meisenheimer complexes, and direct substitution of the nitro group. Thus, we carefully established an initial guess as to the reaction channels of DNAN with •OH based on previous studies [14–18]. High-level DFT calculations were then used to assess the validity of the proposed mechanism. Although a number of assumptions were made with regard to the mechanism, considering the good agreement with previous simulations and experiments, it is believed that the proposed mechanism represents an acceptable hypothesis suitable as a thorough first attempt to theoretically investigate the degradation of DNAN by •OH in AOPs. As in our previous works, we hope that the results obtained from this theoretical simulation can provide strong support for further experimental studies, and valuable help towards finding suitable solutions for explosive pollution.

Computational methods

All stationary points in reaction pathways were fully optimized at the M06-2X/6–311 + G(d,p) level [19, 20], followed by vibrational frequency analysis. For all optimizations, solvation effects was considered synchronously at the same level of theory, using a self-consistent reaction field (SCRF) [21] based on the SMD solvation model [22]. The function M06-2X and the SMD solvation model have been used successfully by Leszczynski's group to study the alkaline hydrolysis of TNT, DNT, DNAN and RDX [14, 16]. Therefore, we did not retestify their reliabilities. Since AOPs are generally carried out in water, we used the dielectric constant of water at 298.0 K, $\varepsilon = 78.4$. The default parameters of the program were used in all computations. Stationary points were further characterized as either local minima (intermediates, no imaginary frequency) or saddle points [transition states (TSs), one and only one imaginary frequency]. The intrinsic reaction coordinates (IRC) [23] path was traced to check the energy profiles connecting each TS to the two associated minima of the proposed mechanism. Additionally, zero-point vibrational energies, and corrections to enthalpy, entropy and Gibbs free-energy were also determined by calculation of the analytic harmonic vibrational frequencies at the same theory level as geometry optimization. The refined energies were corrected to enthalpies and free energies at 298.15 K and 1 atm, using the revised harmonic frequencies. Gibbs free energies of all considered species were calculated using standard expression, $\Delta G = \Delta H - T \cdot \Delta S$, where ΔG is the activation Gibbs free energy, and ΔH and ΔS are the activation enthalpy and entropy, respectively. T is the absolute temperature (298.15 K in this study). All calculations were carried out with the Gaussian 09 suite of programs [24].

Results and discussion

The generation of •OH radicals plays a main role in AOPs, because •OH with an unpaired electron on the oxygen atom is the second strongest oxidant after fluorine. This radical has a very effective standard potential [$E^{o}(\bullet OH/H_2O) = 2.8$ V vs. normal hydrogen electrode (NHE) at pH = 0)], which is able to readily steal hydrogen atoms from other molecules to form water molecules, and add into unsaturated bonds [25]. The reactions between •OH and target compounds in aqueous solution are complex chemical processes that include a number of oxidized radical intermediates. However, the two initial reaction mechanisms—hydrogen abstraction and addition to unsaturated bonds (double bond or aromatic ring)—remain unequivocal [25].

Hydrogen abstraction reactions

Based on previous work [14–18], we designed the complete hydrogen abstraction (H-abstraction) reaction pathways of DNAN; the results are shown in Fig. 1. It is worth noting that we focus mainly on reactions involving only •OH radicals and do not consider other active reactants (such as O_2). Next, we gradually elucidated the details of the H-abstraction reactions of DNAN shown in Fig. 1, including the intermediates and TSs at the very early stage of the reactions and the data of reaction ($\Delta G_R^{\ddagger}$) or activation ($\Delta G^{\ddagger}$) Gibbs free energies.

In general, this route is composed of a series of H-abstraction and dehydration reactions. In the first step, an •OH radical abstracts an H atom from the CH_3 group of DNAN, then produces radical intermediate **1** and a molecule of H_2O by **TS1**. From **TS1** in Fig. 2, we see that the lengths of the C–H breaking and H–O forming bonds are 1.16 Å and 1.45 Å, respectively, which implies that the H-abstraction is an asynchronous atom-transfer reaction and the geometry of the TS is closer to that of the reactant.

The data listed in Table 1 also show that the first H-abstraction reaction need only overcome a low activation energy barrier of 10.8 kcal mol^{-1} and has an exothermicity of 19.2 kcal mol^{-1}. The radical intermediate **1** further reacts with the second •OH without the barrier due to the combination of two radicals, and generates the intermediate compound **2** with a very high exothermicity of 88.5 kcal mol^{-1}. The next step from **2** to **3** is a dehydration reaction with an abnormally high barrier of $\Delta G^{\ddagger} = 80.8$ kcal mol^{-1} (see Table 1). The

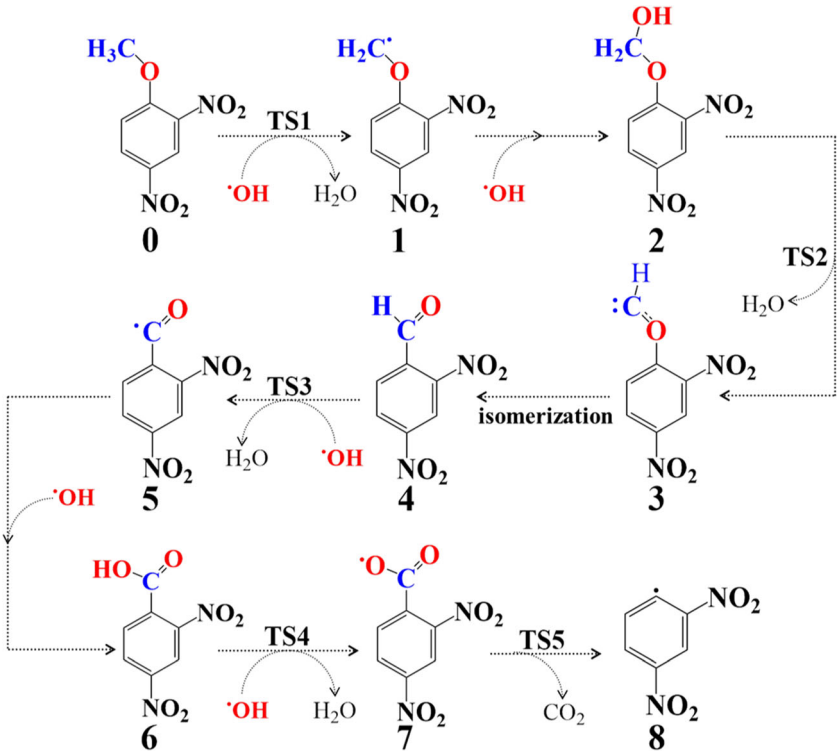

Fig. 1 Hydrogen abstraction reaction mechanisms for degradation reactions of 2,4-dinitrotoluene (DNT) solely by OH• radicals

corresponding **TS2** is closer to the product (H_2O), judging from the length data labeled in Fig. 2. Generally, a reaction with such a high barrier is impossible at room temperature. However, the former two reactions (**0** → **1** and **1** → **2**) had released enough heat (107.7 kcal mol^{-1}) to support the probable occurrence of this dehydration reaction (**2** → **3**). Of course, it is more likely that radical **1** has another choice and, for example, would react with O_2, because radicals such as **1** have relatively low energy barriers for reaction with O_2 [25] and the concentration of •OH is much lower than that of dissolved O_2 [26].

After generating compound **3**, basically there are no reactions with the extra high barrier. First, the formed intermediate **3** with unpaired electrons is indeed unstable, and converts easily into isomer **4**, which is more stable and has higher energy of 71.3 kcal mol^{-1} (see Table 1). The details of just this isomerization reaction (**3** → **4**) are given in Fig. 3. It is clear that there is a relatively short distance of 2.78 Å between the C atom with unpaired electrons and the O atom of the nitro group at the ortho position in **3**. Due to the surplus electrons of the C atom and the high electronegativity of the O atom, the C atom is easily dragged to the O atom, and the last distance is 1.31 Å, which illustrates the formation of a covalent bond. This progress can release heat energy of 31.2 kcal mol^{-1}. In Fig. 3, the generated isomer **3′** is also a temporary intermediate, because it just needs to cross a low barrier of $\Delta G^{\ddagger} = 7.7$ kcal mol^{-1} (corresponding to $\mathbf{TS}_{iso}$), and arrive at a more stable product **4** (2,6-dinitrobenzaldehyde) with an exothermicity of 40.1 kcal mol^{-1}. Similar structures, including benzaldehyde, are also found in the AOPs of TNT [17] and DNT [18].

From Fig. 1, we can see that the next reaction is as same as that of DNT, i.e., intermediate **4** would be further robbed of a

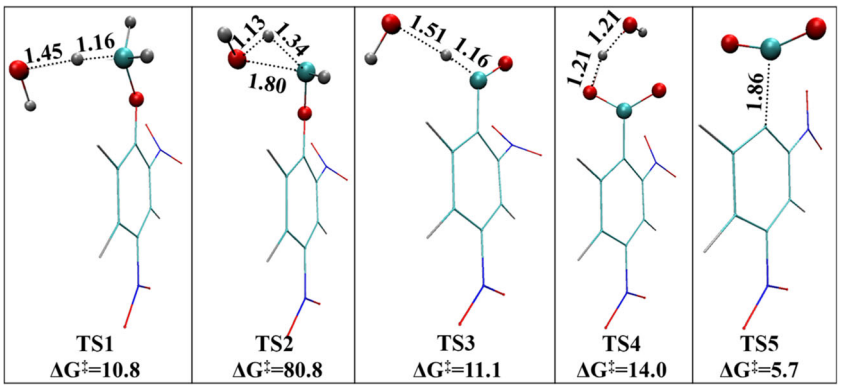

Fig. 2 Optimized geometries of **TS1**, **TS2**, **TS3**, **TS4** and **TS5** for hydrogen abstraction reactions of 2,4-dinitroanisole (DNAN), with the selected distance given in Å. The activation energy is given in kcal mol^{-1}

Table 1 Reaction ($\Delta G_R^{\ddagger}$) and activation ($\Delta G^{\ddagger}$) Gibbs free energies at 298.15 K for all reactions in Fig. 1 (kcal mol^{-1}). The compounds represented by notations are **TS1**–**TS5** are illustrated in Figs. 1 and 2

Reaction step	$\Delta G_R^{\ddagger}$	$\Delta G^{\ddagger}$	Reaction step	$\Delta G_R^{\ddagger}$	$\Delta G^{\ddagger}$
0 + •OH → **TS1** → **1** + H_2O	−19.2	10.8	**4** + •OH → **TS3** → **5** + H_2O	−40.5	11.1
1 + •OH → **2**	−88.5	~	**5** + •OH → **6**	−84.1	~
2 → **TS2** → **3** + H_2O	57.8	80.8	**6** + •OH → **TS4** → **7** + H_2O	−3.1	14.0
3 → **4** (isomerization)	−71.3	7.7	**7** → **TS5** → **8** + CO_2	−16.8	5.7

hydrogen by the third attack of •OH. The corresponding **TS3**, which is closer to the reactant like **TS1** based on the labeled length, has a barrier of 11.1 kcal mol^{-1} and leads to radical intermediate **5**. Then, **5** would continue to combine with a •OH radical to generate 2,4-dinitrobenzoic acid (**6**) with the large heat output of $\Delta G_R^{\ddagger} = -84.1$ kcal mol^{-1}. Then, again through an H-abstraction, compound **6** is transformed into radical intermediate **7** by **TS4**. The low barrier ($\Delta G^{\ddagger} =$ 14.0 kcal mol^{-1}) indicates that this H-abstraction reaction also occurs easily at room temperature. As a TS of the H-abstraction reaction, **TS4** is slightly different to the previous two, i.e., **TS1** and **TS3**. For the geometry of **TS4** shown in Fig. 2, the C–H bond of the carboxyl group is stretched to 1.21 Å, which is equal to the O–H bond length of the hydroxyl radical. Crossing a very low barrier of 5.7 kcal mol^{-1}, radical **7** removes carbon dioxide by **TS5** and finally produces the other radical intermediate, **8**. Due to the conjugative effect of the benzene ring, radical **8** is relatively stable, and easily captures an H-atom to form 1,3-dinitrobenzene. A similar process involving a series of H-abstraction reactions can also be called methyl oxidation in AOPs of TNT [17] and DNT [18], with the final product generally being 1,3,5-trinitrobenzene and 1,3-dinitrobenzene, respectively. By comparison, DNAN has an extra oxygen atom between the methyl group and the benzene ring, which results in only one additional isomerization reaction. Furthermore, the isomerization reaction is a highly exothermic process ($\Delta G_R^{\ddagger} = -71.2$ kcal mol^{-1}), and needs only to overcome a small energy barrier ($\Delta G^{\ddagger} =$ 7.7 kcal mol^{-1}). Therefore, as for TNT and DNT, the H-abstraction reaction details described in this work should be one of the important degradation mechanisms of DNAN by AOPs.

Addition reactions to aromatic rings

Generally, the addition reaction is one of the main processes involving •OH in the presence of aromatic compounds, and this reaction can be very fast, and is sometimes controlled by diffusion [27]. In subsequent investigations, we focused mainly on the addition reactions of •OH radical to aromatic rings. The six carbon atoms in the benzene ring are numbered **I**–**VI** in sequence, as shown in the bottom right corner of Fig. 4. If we consider only the addition of a single •OH radical, the total molecular energies and geometries of six isomeric intermediates (**9**–**14**) are given in Fig. 4. We found that, when C atoms (**I**, **II**, **IV**, and **VI**) with a substituent (nitro- or methyl ether group) are added by •OH, the energy of the radical adducts generated is relatively lower than that from a C atom (**III** and **V**) without the substituent. For example, based on the total molecular energy, radical **10** ($\Delta G = -17.0$ kcal mol^{-1}) should be the most stable additive product. We selected the first two

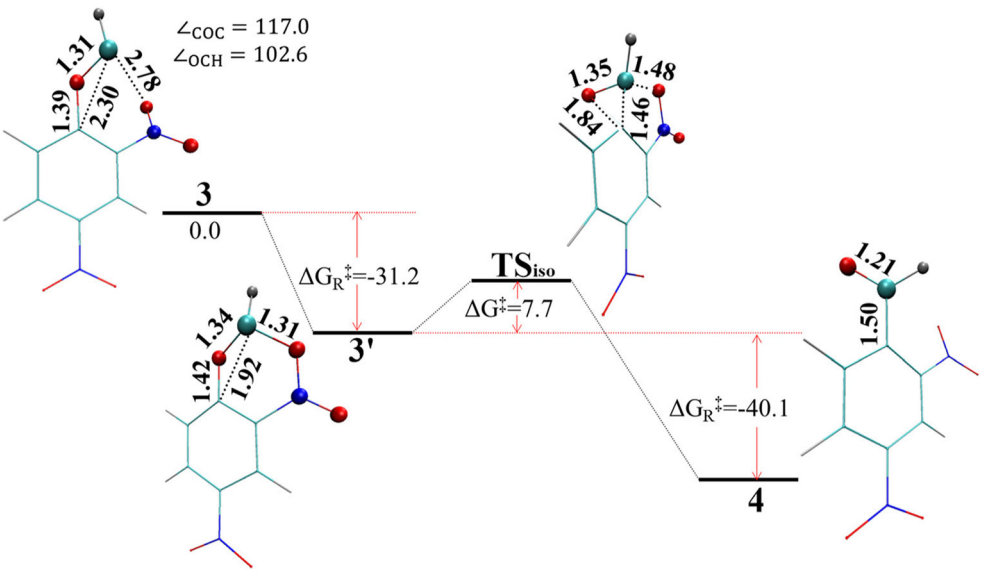

Fig. 3 Free-energy profiles and transitions state (TS) geometries for the isomerization reaction of the intermediate **3** from H-abstraction reaction. Distances are in Å; activation energies are in kcal mol^{-1}

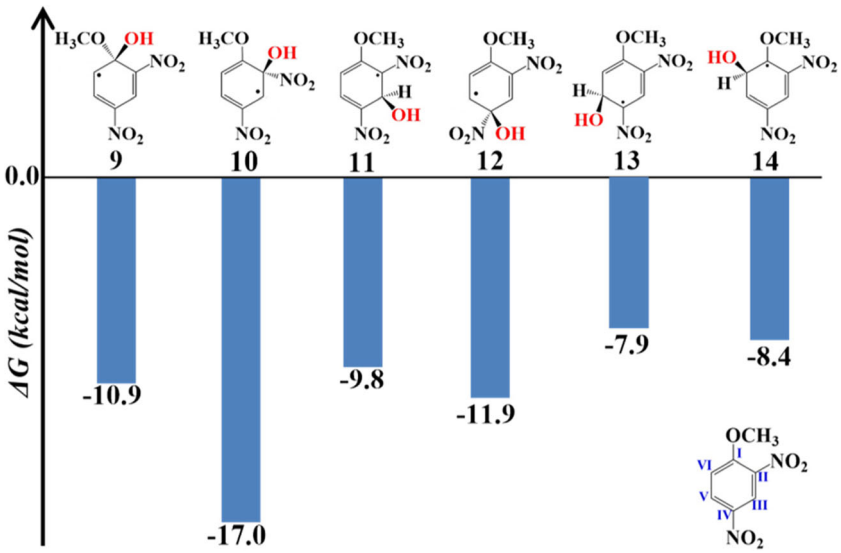

Fig. 4 Difference in free energy (ΔG) for six addition products (**9**–**14**). Reference energy (0.0 kcal mol^{-1}) is the sum of that of DNAN and the •OH radical

additive products, i.e., **9** and **10**, as examples to explore the following reactions (see Fig. 5).

Based on our previous work [17, 18] and a reported work on toluene [28], we know that the direct substitution pathway (addition-elimination mechanism) has an advantage in terms of thermodynamics. For the first addition product **9** in Fig. 5, we find that the addition-elimination reaction (departure of a single CH_3O• radical) occurs easily with a barrier of $\Delta G^{\ddagger}$ = 18.0 kcal mol^{-1}, which is slightly higher than that of the previous H-abstraction reaction ($\Delta G^{\ddagger}$ = 10.8 kcal mol^{-1}). Energy (−10.9 kcal mol^{-1}) released by the addition process of the •OH radical to the aromatic ring can easily make up the gap. Theoretically, this should represent the competitive reaction of the H-abstraction, if the effect of energy dissipation and steric hindrance is not considered. As for the second addition product **10**, its elimination process of •NO_2 radical is almost no barrier ($\Delta G^{\ddagger}$ = 0.1 kcal mol^{-1}) and, however, gives out heat of 21.0 kcal mol^{-1}.

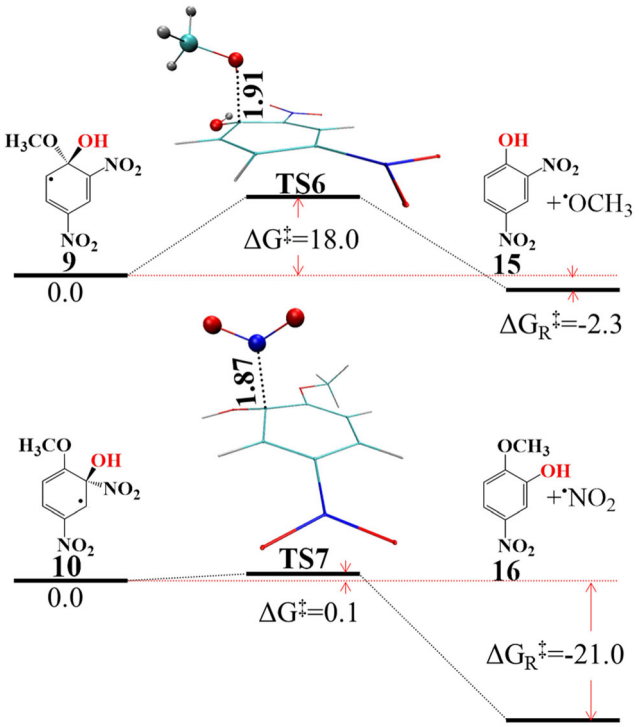

Fig. 5 Free-energy profiles and TS geometries of the addition-elimination reaction (one •OH radical) for products **9** and **10**. Distances in Å, activation energies in kcal mol^{-1}

The same products (**15** and **16**) can also be obtained from the addition of two •OH radicals followed by an elimination reaction, as shown in Fig. 6. For the addition products of two •OH, **17** and **18**, their total energies decline by 58.6 kcal mol^{-1} and 59.9 kcal mol^{-1}, respectively, which seems to favor this pathway. However, the subsequent elimination reaction requires a very high energy barrier. In detail, the elimination of formic acid (CH_3COOH) by **TS8** needs to overcome a barrier of 104.2 kcal mol^{-1}, and the elimination of nitric acid (HNO_3) by **TS9** also has a barrier of 70.6 kcal mol^{-1}. The previous reactions do not release enough heat to overcome the high barrier of the elimination reactions. It is very clear that these hydroxyl substituted products (like **15** and **16**) are generated mainly from the addition-elimination reaction mechanism based on the reaction barriers. It is worth emphasizing that the so-called addition process is the addition of a single hydroxyl radical.

Denitration reactions

In AOPs of TNT [29] and DNT [8], denitration products, such as dinitrotoluene, mononitrotoluene, and dinitrobenzene, are often detected. Our previous studies on TNT and DNT did not conduct an in-depth investigation of this reaction. Here, we take DNAN as an example to explore the possible mechanism of denitration reactions. Early studies on the nitromethane

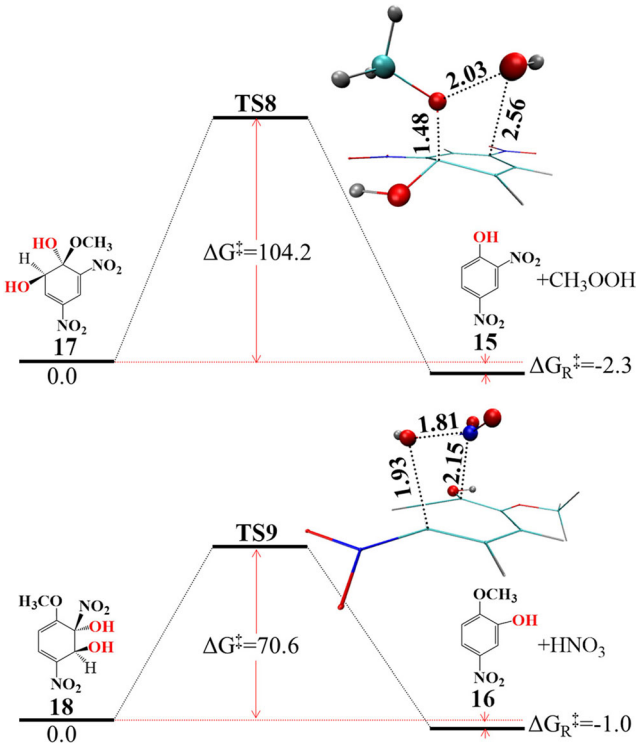

Fig. 6 Free-energy profiles and TS geometries of the addition-elimination reaction (two •OH radicals) for products **17** and **18**. Distances are in Å; activation energies are in kcal mol^{-1}

decomposition reaction stated that isomerization of the nitro group is a possible channel [30]. Therefore, we first explored the isomerization reaction of the nitro group at the **IV** position for DNAN, as shown in Fig. 7. Compared with DNAN (**0**), there is no obvious change in the energy of the isomerization product **19** ($\Delta G_R^{\ddagger}$ = 1.8 kcal mol^{-1}). However, **TS11** has an activation energy barrier of $\Delta G^{\ddagger}$ = 67.9 kcal mol^{-1}, which is relatively high. Because of this high barrier, Zeman et al. [31] believed that the initial reaction of nitromethane was C–N bond cleavage, rather than isomerization of the nitro group. In addition, from Fig. 7, we can see that product **19** has an elongated N–O bond that is 1.41 Å more than the other N–O bond (1.16 Å). When the ONO group of **19** is further attacked by an •OH radical, this reaction overcomes only a relatively low barrier ($\Delta G^{\ddagger}$ = 14.3 kcal mol^{-1}) to form a benzoquinone radical **20** by leaving a nitrous acid (HNO_2). This is an exothermic reaction ($\Delta G_R^{\ddagger}$ = 34.9 kcal mol^{-1}). It is interesting that a similar benzoquinone intermediate (**20′**) is also found in the next step of the direct substitution product (**16**) of the •OH radical (that is, from the addition-elimination mechanism). The corresponding results are given in Fig. 8.

As shown in Fig. 8, when an •OH radical is close to the H-atom of the phenol hydroxyl group, the H-abstraction reaction would occur via **TS13**. It must be emphasized that this H-abstraction reaction is almost no energy barrier. In fact, Fig. 8 gives the IRC path based on **TS13** at the B3LYP/6–31 + G** level. If the calculation level is raised to the M06-2X/6–311 + G** level, the TS cannot be found. In Fig. 8, it is clear that the pathway from **16** to **TS13** is exceptionally flat. Formation of the benzoquinone radical **20′** is a highly exothermic process. On the other hand, the •OH radical can also get another hydrogen atom from the anisole group, which has a relatively high barrier of $\Delta G^{\ddagger}$ = 13.0 kcal mol^{-1}. Obviously, the next pathway after the addition-elimination reaction should have two competing choices. If other factors are not considered, H-abstraction from the phenol hydroxyl group should prevail. This may be the reason that intermediates of the benzoquinone radical are often detected. It is also in agreement with experimental results [29, 32], which detected several benzoquinone radicals. The isomerization mechanism of the nitro group resulting in formation of the benzoquinone radical cannot be completely ruled out, because the nitro isomerization always occurs under conditions of illumination [33]. Moreover, the subsequent reaction with •OH can generate the benzoquinone radical through a relatively low barrier. Agreeing with the above point, Liou et al. [29] found the benzoquinone radical under photo-Fenton conditions. Regarding the subsequent reactions of benzoquinone radicals, we will investigate them in the future due to their extreme complexity.

At this point, the reaction mechanisms of nitro isomerization that are originally designed for denitration have resulted in the formation of benzoquinone radicals. Although benzoquinone radicals are often detected in several experiments,

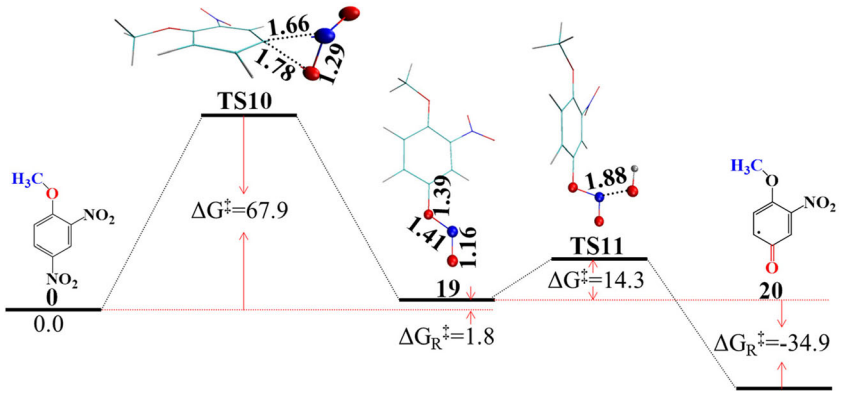

Fig. 7 Free-energy profiles and TS geometries of the isomerization reaction of the nitro group. Distances are in Å; activation energies are in kcal mol^{-1}

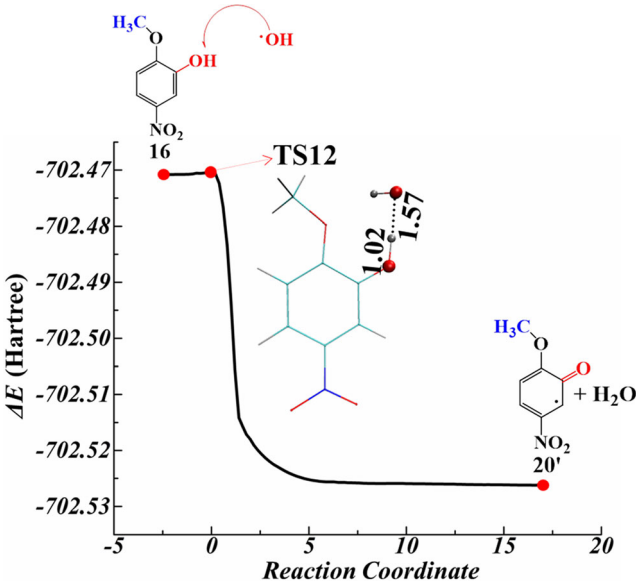

Fig. 8 Free-energy profiles along with the intrinsic reaction coordinates (IRC) reaction path for the reaction from **16** to **20′** by **TS12**

they still might have come from other reactions. In fact, if limited only to reactions related to •OH radicals, the denitration reaction is almost impossible. Hence, we consider the participation of other reactive substances. Among them, the simplest mechanism is the direct substitution of hydrogen radicals ($H^+ + e \rightarrow$ •H). The above mentioned study had indicated that the addition product (**10**) of •OH to the **II** position is most stable, because of the lowest energy of $\Delta G_R^{\ddagger} = -17.0$ kcal mol^{-1}. Therefore, the addition intermediate (**21**) of •H to the **II** position was considered first, and has a greater energy drop than **10** ($\Delta G_R^{\ddagger} = -25.9$ kcal mol^{-1}). Like **10**, addition product **21** may also induce a sustainable reaction based on the addition-elimination mechanism, and finally form denitration product **22** through **TS14** (see Fig. 9). This step of the reaction has only a very low barrier of 2.1 kcal mol^{-1} but can emit heat of 21.4 kcal mol^{-1}. Clearly, this mechanism is also applicable to denitration reactions of other nitroaromatic explosives such as TNT and DNT. Of course,

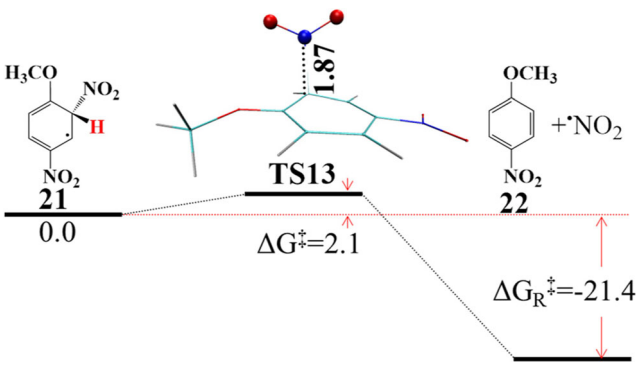

Fig. 9 Free-energy profiles and TS geometry for the addition-elimination reaction of the nitro group and hydrogen radical (•H). Distance are in Å; activation energies are in kcal mol^{-1}

the probability of this reaction depends mainly on the concentration of •H radicals (i.e., production speed and duration) in the Fenton reaction.

Comparison

One of the primary concerns with explosives degradation by AOPs is that the final products and intermediates may in some cases still be toxic, possibly even more toxic than the parent compound [1]. An in-depth and detailed understanding of the degradation mechanisms can help us identify the final products and intermediates of AOPs. On the basis of the above studies, the potential energy surfaces of the four possible reaction pathways are summarized in Fig. 10, allowing us to compare them as a whole. The first is the H-abstraction reaction, which just needs to climb an energy barrier of $\Delta G^{\ddagger} =$ 10.8 kcal mol^{-1} and then goes downhill. Such a low barrier ensures that the reaction can take place at room temperature. Notably, the subsequent dehydration reaction from **2** to **3** with a high barrier ($\Delta G^{\ddagger} = 80.8$ kcal mol^{-1}) sets up an obstacle to the whole H-abstraction pathway. However, the first two steps of the reaction (**0** → **1** and **1** → **2**) release enough heat to support the sustained response. Additionally, under real conditions, this step may be skipped by the participation of active oxygen, like for TNT [34]. Compared with TNT [17] and DNT [18], the H-abstraction reactions of DNAN increase one-step isomerization (that is, **3** → **4** in Fig. 4). However, they do not influence the whole progress.

As for addition-elimination mechanisms, the addition of two •OH radicals to the benzene ring will decrease the energy of the products more than that of one •OH radical. For example, the energy of the double addition product **17** drops to −58.6 kcal mol^{-1}, and the single addition product **10** is decreased by −17.0 kcal mol^{-1}. However, the subsequent elimination reaction for **17** has a very high barrier of $\Delta G^{\ddagger} =$ 104.2 kcal mol^{-1}, which is far more than that for **10** (0.1 kcal mol^{-1}). Excluding the heat from the previous step, the remaining barrier of 45.6 kcal mol^{-1} is still difficult to overcome. Obviously, the addition-elimination reaction mediated by a single •OH radical is the dominate mechanism. The corresponding phenol products are also easily robbed of an H atom from the phenol group by other •OH radicals, which is almost no barrier (see Fig. 8). The formed benzoquinone radical can destroy the conjugated benzene ring. Maybe this is one of the ring opening reaction mechanisms. Another source of the benzoquinone radical is the departure of nitrous acid (HNO_2) after isomerization of the nitro group. This reaction is more likely to occur under illumination conditions.

Judging from the present results, the denitration reaction must include the participation of reactive reactants other than •OH radicals. Here, we assume the participation of •H radicals. Then, this reaction, which also uses the addition-elimination mechanism, will obtain the denitration product

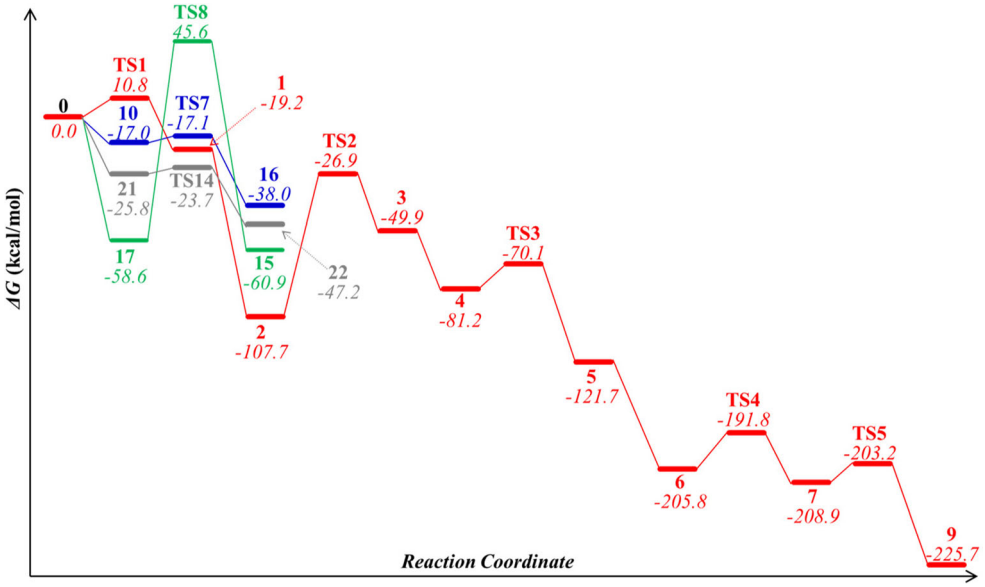

Fig. 10 Relative ΔG potential energy surfaces for the degradation reaction pathways of DNAN (kcal mol^{-1}). The compounds represented by the notations can be seen in Figs. 1–9

22 easily through a relative low barrier of $\Delta G^{\ddagger}$ = 2.1 kcal mol^{-1}. The addition process may also be carried out in two steps, i.e., a hydrogen proton (H^+) is first added to the benzene ring, and then the cationic complex formed is combined with an electron (*e*). H^+ and *e* are common products of the Fenton process (or AOPs).

Conclusions

In summary, the detailed degradation reaction mechanism of a typical insensitive explosive, DNAN, by hydroxyl radicals in AOPs has been studied initially with DFT methods at the M06-2X/6–311 + G(d,p)/SMD level. The main conclusion of this work can be summarized as follows: for AOP degradation of DNAN, the representative degradation mechanism is mainly the H-abstraction reaction and the direct substitution (or addition-elimination) of the nitro group. Due to the deficiency of experimental data for DNAN, it is not possible to complete a detailed comparison between computational and experimental results. However, Leszczynski et al. [16] found similar phenomena in the alkali hydrolysis of DNAN, i.e., the predominant product came from the reaction of demethylation and direct substitution of a nitro group by a hydroxide anion. The mechanism of addition-elimination is more crucial in this process due to the very low energy barrier. As for the H-abstraction reaction, it is only one possible competing pathway. The direct substitution product from the addition-elimination mechanism can further produce a benzoquinone radical through an H-abstraction process without the barrier. Isomerization of the nitro group has a barrier of 67.9 kcal mol^{-1}, and can also bring a benzoquinone radical intermediate. Comparing experimental data [32], we think that this reaction may occur only under light conditions. The denitration reaction does not result from the participation of only •OH radicals; other active reactants, such as •H radical, may be involved. In addition, details of TSs, intermediate radicals and free energy surfaces for all proposed reactions are given and make up for a lack of experimental knowledge. On the whole, the degradation mechanisms of DNAN by AOPs are very similar to those of TNT and DNT, including intermediates and thermodynamics information. As with disposal of TNT and DNT, the removal of DNAN utilizing AOPs seems a good choice.

Acknowledgments All the authors appreciate very much the financial support from President Foundation of China Academy of Engineering and Physics(CAEP; No. 2014-1-075) and Sichuan University of Science and Engineering Foundation (No. 2015RC28).

References

1. Sunahara GI, Lotufo G, Kuperman RG, Hawari J (2009) Ecotoxicology of explosives. CRC, Boca Raton
2. Davies PJ, Provatas A (2006) Characterisation of 2,4-dinitroanisole: an ingredient for use in low sensitivity melt cast formulations. DTIC Document. Weapons Systems Division , Defence Science and Technology Organisation, Edinburgh, Australia
3. Boddu VM, Abburi K, Maloney SW, Damavarapu R (2008) Thermophysical properties of an insensitive munitions compound, 2,4-dinitroanisole. J Chem Eng Data 53:1120–1125
4. Arnett CM, Rodriguez G, Maloney SW (2009) Analysis of bacterial community diversity in anaerobic fluidized bed bioreactors treating 2,4-dinitroanisole (DNAN) and n-methyl-4-nitroaniline (MNA) using 16S rRNA gene clone libraries. Microbes Environ 24:72–75
5. Ayoub K, Nélieu S, Van Hullebusch ED et al (2011) Electro-Fenton removal of TNT: evidences of the electro-chemical reduction contribution. Appl Catal B Environ 104:169–176

6. Ayoub K, Nélieu S, Van Hullebusch ED et al (2011) TNT oxidation by Fenton reaction: reagent ratio effect on kinetics and early stage degradation pathways. Chem Eng J 173:309–317
7. Ayoub K, van Hullebusch ED, Cassir M, Bermond A (2010) Application of advanced oxidation processes for TNT removal: a review. J Hazard Mater 178:10–28
8. Chen W-S, Liang J-S (2009) Electrochemical destruction of dinitrotoluene isomers and 2,4,6-trinitrotoluene in spent acid from toluene nitration process. J Hazard Mater 161:1017–1023
9. Yardin G, Chiron S (2006) Photo–Fenton treatment of TNT contaminated soil extract solutions obtained by soil flushing with cyclodextrin. Chemosphere 62:1395–1402
10. Perreault NN, Manno D, Halasz A et al (2012) Aerobic biotransformation of 2,4-dinitroanisole in soil and soil *Bacillus* sp. Biodegradation 23:287–295
11. Platten WE, Bailey D, Suidan MT, Maloney SW (2010) Biological transformation pathways of 2,4-dinitro anisole and N-methyl paranitro aniline in anaerobic fluidized-bed bioreactors. Chemosphere 81:1131–1136
12. Olivares C, Liang J, Abrell L et al (2013) Pathways of reductive 2, 4-dinitroanisole (DNAN) biotransformation in sludge. Biotechnol Bioeng 110:1595–1604
13. Khan F, Pal D, Ghosh A, Cameotra SS (2013) Degradation of 2,4-dinitroanisole (DNAN) by metabolic cooperative activity of pseudomonas sp. strain FK357 and *Rhodococcus imtechensis* strain RKJ300. Chemosphere 93:2883–2888
14. Hill FC, Sviatenko LK, Gorb L et al (2012) DFT M06-2X investigation of alkaline hydrolysis of nitroaromatic compounds. Chemosphere 88:635–643
15. Salter-Blanc AJ, Bylaska EJ, Ritchie JJ, Tratnyek PG (2013) Mechanisms and kinetics of alkaline hydrolysis of the energetic nitroaromatic compounds 2,4,6-trinitrotoluene (TNT) and 2,4-dinitroanisole (DNAN). Environ Sci Technol 47:6790–6798
16. Sviatenko L, Kinney C, Gorb L et al (2014) Comprehensive investigations of kinetics of alkaline hydrolysis of TNT (2,4,6-trinitrotoluene), DNT (2,4-dinitrotoluene), and DNAN (2,4-dinitroanisole). Environ Sci Technol 48:10465–10474
17. He X, Zeng Q, Zhou Y et al (2016) A DFT study toward the reaction mechanisms of TNT with hydroxyl radicals for advanced oxidation processes. J Phys Chem A 120:3747–3753
18. Zhou Y, Yang Z, Yang H et al (2017) Reaction mechanisms of DNT with hydroxyl radicals for advanced oxidation processes—a DFT study. J Mol Model 23:139
19. Zhao Y, Truhlar DG (2008) The M06 suite of density functionals for main group thermochemistry, thermochemical kinetics, noncovalent interactions, excited states, and transition elements: two new functionals and systematic testing of four M06-class functionals and 12 other functionals. Theor Chem Accounts 120: 215–241
20. McLean AD, Chandler GS (1980) Contracted Gaussian basis sets for molecular calculations. I. Second row atoms, Z= 11–18. J Chem Phys 72:5639–5648
21. Simkin BI, Sheĭkhet II (1995) Quantum chemical and statistical theory of solutions: a computational approach. Ellis Horwood, London
22. Marenich AV, Cramer CJ, Truhlar DG (2009) Universal solvation model based on solute electron density and on a continuum model of the solvent defined by the bulk dielectric constant and atomic surface tensions. J Phys Chem B 113:6378–6396
23. Hratchian HP, Schlegel HB (2004) Accurate reaction paths using a hessian based predictor–corrector integrator. J Chem Phys 120: 9918–9924
24. Bearpark M, Heyd JJ, Brothers E et al (2009) Gaussian 09, Revision A 01. Gaussian, Wallingford
25. Gligorovski S, Strekowski R, Barbati S, Vione D (2015) Environmental implications of hydroxyl radicals (•OH). Chem Rev 115:13051–13092
26. Krasnovsky AA (2007) Primary mechanisms of photoactivation of molecular oxygen. History of development and the modern status of research. Biochemistry 72:1065–1080
27. Buxton GV, Greenstock CL, Helman WP, Ross AB (1988) Critical review of rate constants for reactions of hydrated electrons, hydrogen atoms and hydroxyl radicals (·OH/·O)− in aqueous solution. J Phys Chem Ref Data 17:513–886
28. Hatipoglu A, Vione D, Yalçın Y et al (2010) Photo-oxidative degradation of toluene in aqueous media by hydroxyl radicals. J Photochem Photobiol A Chem 215:59–68
29. Liou M-J, Lu M-C, Chen J-N (2004) Oxidation of TNT by photo-Fenton process. Chemosphere 57:1107–1114
30. Michale LM (1986) Ab initio study of rearrangements on the nitromethane potential energy surface. J Am Chem Soc 108:784–785
31. Zeman S, Atalar T, Friedl Z, Ju X-H (2009) Accounts of the new aspects of nitromethane initiation reactivity. Cent Eur J Energetic Mater 6:119–133
32. Hess TF, Renn TS, Watts RJ, Paszczynski AJ (2003) Studies on nitroaromatic compound degradation in modified Fenton reactions by electrospray ionization tandem mass spectrometry (ESI-MS-MS). Analyst 128:156–160
33. Zhang C, Chen M, Wang G et al (2012) Photo-induced isomerization of three nitrotoluene isomers: a matrix-isolation infrared spectroscopic and quantum-chemical study. Chem Phys 392:198–204
34. Schmelling DC, Gray KA (1995) Photocatalytic transformation and mineralization of 2,4,6-trinitrotoluene (TNT) in TiO_2 slurries. Water Res 29:2651–2662